

Long-term Brain Tissue Monitoring after Semi-brain Irradiation in Rats Using Proton Magnetic Resonance Spectroscopy: A Preliminary Study *In vivo*

Hong Chen¹, Yu-Shu Cheng², Zheng-Rong Zhou¹

¹Department of Radiology, Fudan University Shanghai Cancer Center; Department of Oncology, Shanghai Medical College, Fudan University, Shanghai 200032, China

²Department of Radiology, Eye and ENT Hospital of Fudan University, Shanghai 200031, China

Hong Chen and Yu-Shu Cheng contributed equally to this work

Abstract

Background: In head and neck neoplasm survivors treated with brain irradiation, metabolic alterations would occur in the radiation-induced injury area. The mechanism of these metabolic alterations has not been fully understood, while the alternations could be sensitively detected by proton (¹H) nuclear magnetic resonance spectroscopy (MRS). In this study, we investigated the metabolic characteristics of radiation-induced brain injury through a long-term follow-up after radiation treatment using MRS *in vivo*.

Methods: A total of 12 adult Sprague-Dawley rats received a single dose of 30 Gy radiation treatment to semi-brain (field size: 1.0 cm × 2.0 cm; anterior limit: binocular posterior inner canthus connection; posterior limit: external acoustic meatus connection; internal limit: sagittal suture). Conventional magnetic resonance imaging and single-voxel ¹H-MRS were performed at different time points (in month 0 before irradiation as well as in the 1st, 3rd, 5th, 7th, and 9th months after irradiation) to investigate the alternations in irradiation field. N-acetylaspartate/choline (NAA/Cho), NAA/creatinine (Cr), and Cho/Cr ratios were measured in the bilateral hippocampus and quantitatively analyzed with a repeated-measures mixed-effects model and multiple comparison test.

Results: Significant changes in the ratios of NAA/Cho ($F = 57.37$, $P_g < 0.001$), NAA/Cr ($F = 54.49$, $P_g < 0.001$), and Cho/Cr ($F = 9.78$, $P_g = 0.005$) between the hippocampus region of the irradiated semi-brain and the contralateral semi-brain were observed. There were significant differences in NAA/Cho ($F = 9.17$, $P_t < 0.001$) and NAA/Cr ($F = 13.04$, $P_t < 0.001$) ratios over time. The tendency of NAA/Cr to change with time showed no significant difference between the irradiated and contralateral sides. Nevertheless, there were significant differences in the Cho/Cr ratio between these two sides.

Conclusions: MRS can sensitively detect metabolic alternations. Significant changes of metabolites ratio in the first few months after radiation treatment reflect the metabolic disturbance in the acute and early-delayed stages of radiation-induced brain injuries.

Key words: Proton Magnetic Resonance Spectroscopy; Radiation Injuries; Radiotherapy; Rats

INTRODUCTION

Although recent advances in radiation techniques have made radiation safer for the tissues distant to a tumor, the exposure of healthy brain tissue to radiation cannot be completely eliminated. As the tumor bed receives the highest dose of radiation, the surrounding normal brain tissues would also suffer more radiation exposure. According to the time interval between radiation exposure and the injury, radiation-induced central nervous system injury is classified into acute, early delayed, and late delayed stages. Radiation-induced brain injury is one of the most serious complications of radiation

therapy, which can lead to devastating functional deficits, such as headaches, nausea, emesis, somnolence, stroke-like

Address for correspondence: Dr. Zheng-Rong Zhou, Department of Radiology, Fudan University Shanghai Cancer Center; Department of Oncology, Shanghai Medical College, Fudan University, Shanghai 200032, China
E-Mail: zhouzr-16@163.com

This is an open access article distributed under the terms of the Creative Commons Attribution-NonCommercial-ShareAlike 3.0 License, which allows others to remix, tweak, and build upon the work non-commercially, as long as the author is credited and the new creations are licensed under the identical terms.

For reprints contact: reprints@medknow.com

© 2017 Chinese Medical Journal | Produced by Wolters Kluwer - Medknow

Received: 15-10-2016 **Edited by:** Ning-Ning Wang
How to cite this article: Chen H, Cheng YS, Zhou ZR. Long-term Brain Tissue Monitoring after Semi-brain Irradiation in Rats Using Proton Magnetic Resonance Spectroscopy: A Preliminary Study *In vivo*. Chin Med J 2017;130:957-63.

Access this article online

Quick Response Code:



Website:
www.cmj.org

DOI:
10.4103/0366-6999.204097

migraine attacks after radiation therapy syndrome, and even brain necrosis, that would persist months or years after radiation therapy.^[1-3] However, those symptoms are common and nonspecific. Normally, the treatment for radiation injury could only be symptomatic therapy, which is insufficient. An accurate and sensitive detection on radiation-induced brain injury is necessary for modifying treatment strategies and thereby minimizing possible injuries. The effects of radiation on normal living human brain tissue can be delineated using *in vivo* proton magnetic resonance spectroscopy (¹H-MRS). This kind of spectroscopy could be applied not only to noninvasively measure human brain metabolites, but also to monitor head and neck neoplasm treatment responses after radiotherapy.^[2,4-6] Unfortunately, rare animal studies have been performed to explore the metabolic alterations that occur in the brain over time after radiation therapy. In general, postoperative observation period is extremely short, and the dynamic changes of the MRS metabolic values in a long period after radiation are still unclear.^[6] This study evaluated the metabolic changes in rat brains after half-brain irradiation within a postirradiation period of up to nine months using ¹H-MRS.

METHODS

Animal preparation

A total of 12 adult male Sprague-Dawley rats (12 weeks old, mean weight: 270 ± 30 g) were involved in the present study. The observation time points included a measurement time (month 0) before radiation treatment and those (1st, 3rd, 5th, 7th, and 9th months) after radiation treatment. In both irradiation and magnetic resonance imaging (MRI) scans, all animal experiment procedures were performed under general anesthesia using 10% chloral hydrate anesthesia (Sinopharm Chemical Reagent Co., Ltd., Shanghai, China, 0.4 ml/100 g body weight, intraperitoneal [i.p.] injection). In histopathological evaluation, 10% chloral hydrate anesthesia i.p. injection was performed for deep anesthesia before perfusion fixation. All efforts were made to minimize animal suffering. All animal handling and experimental protocols conformed to *the Guiding Directive for Humane Treatment of Laboratory Animals* issued by the Chinese National Ministry of Science and Technology. All experiments were approved by the Shanghai Medical Experimental Animal Administrative Committee (No. 2009-0082).

Under 10% chloral hydrate anesthesia, rats were irradiated in brain hemisphere (right side: $n = 6$; left side: $n = 6$) with a highly collimated 6 MV photon beam from a linear accelerator (Primus-M, Siemens, Germany) with a single dose of approximately 30 Gy. The animal model of the irradiation treatment to brain hemisphere for the longitudinal evaluation of radiation-induced brain injury using a magnetic resonance (MR) scanner was utilized in previous studies.^[7,8] To avoid radiation injury, the whole bodies of rats, except the irradiated region, were protected by lead leather, which served as an internal control side for the subsequent analyses.

A single dose of 30 Gy was given to rats because it was known to be the minimum required dose to produce selective late necrosis in some regions of rat brain without causing death or detectable neurological changes.^[7,9] All animals were irradiated with a source having a surface distance of 80 cm from the center of the animal with a field size of 1.0 cm × 2.0 cm (former limit: binocular posterior inner canthus connection; posterior limit: external acoustic meatus connection; and internal limit: sagittal suture).

Magnetic resonance imaging scanning protocol

MRI was performed using a 3 Tesla MRI system (Verio 3T, Siemens, Germany). A four-channel rat brain array coil (Shanghai Chenguang, Shanghai, China) was used for signal reception. Proton MR spectroscopy (¹H-MRS) and T2-weighted imaging (T2WI) were performed on animal brain at different time points. The conventional MRI scan included both axial and coronal T2WI. Imaging parameters were as follows: T2WI was performed using fast spin echo sequences (repetition time [TR]/echo time [TE]: 2680 ms/74 ms; slice thickness: 2.2 mm; spacing: 0.22 mm; matrix size: 232 × 256; field of view: 73 mm × 80 mm; four repetitions; total scan time: 5.3 min).

During ¹H-MRS scanning, we selected rat hippocampus as the field of interest because the incidence of white matter (WM) damage was higher in the fimbria of rat hippocampus as reported in another study.^[10] MRS imaging was carried out using a three-dimensional (3D), multi-voxel, spectroscopic imaging acquisition mode. The water signal was suppressed with a selective water signal inversion. ¹H-MRS scanning started when the full width at half maximum was between 41 Hz and 53 Hz and the water suppression (WS) was ≥98%. A point-resolved spectroscopy sequence was used for signal acquisition (TR/TE: 1700 ms/30 ms; spectral bandwidth: 1.2 kHz; field of view: 70 mm × 70 mm; volume of interest: 30 mm × 30 mm; voxel thickness: 5 mm; phase encoding: 32 × 32; single voxel: 2.2 mm × 2.2 mm × 5.0 mm; two repetitions; the total scan time of each MRS study: 8.4 min).

Data analysis

The 3D MR spectroscopy data were processed offline using standard software (NUMARIS/4, Syngo MR, Siemens Medical Systems, German) in a workstation, which could calculate metabolite values automatically from the area under each metabolite peak. After WS, chemical shifts were referenced to the signal intensity of metabolites (N-acetylaspartate [NAA] at 2.02 part per million [ppm], creatinine (Cr) at 3.01 ppm, and Cho at 3.22 ppm). Metabolic ratios were calculated for NAA/choline (Cho), NAA/Cr, and Cho/Cr. To identify that the whole brain had no abnormal signal intensities in the T2WI sequence, the bilateral cortex-hippocampus regions of brain were selected as the region of interest, with a selected voxel of 2.2 mm × 2.2 mm × 5.0 mm. The analysis of each selected voxel position was kept consistent as far as possible.

Histology

Four experimental rats were sacrificed for the histopathological

evaluation after the final (the 9th month after radiation) MRI scans. They underwent left ventricular perfusion with normal saline and 4% paraformaldehyde. Subsequently, their brains were removed and fixed in 4% formalin. These samples were then embedded, under vacuum, in paraffin wax. Later, the brains were cut into sections of 4 μm and stained with hematoxylin and eosin (HE) for the examination of general morphology. Immunohistochemistry (IHC) staining of glial fibrillary acidic protein (GFAP), a marker for gliosis, was also applied. The presence of pathological characteristics was evaluated by a pathologist who was blinded to the groups.

Statistical analysis

Data were presented as mean \pm standard deviation (SD). A repeated-measures mixed-effects model was utilized to compare the differences in NAA/Cr, NAA/Cho, and Cho/Cr ratios between the control and irradiated brain hemispheres. If repeated measurement test showed statistically significant differences, the data would undergo further statistical tests (multiple comparisons) using *t*-test (between groups) or paired *t*-test (within group). Bonferroni method was applied in multiple comparisons for α correction. All statistical analyses were performed using SPSS software (Version 22.0, IBM SPSS Statistics Inc., Chicago, Illinois, USA). Data were plotted using GraphPad Prism 6.0 (GraphPad Software, San Diego, CA, USA). A two-sided value of $P < 0.05$ was considered to be statistically significant in repeated-measures mixed-effects model test. The *t*-test was deemed to be statistically significant when $P < 0.008$ (0.05/6).

RESULTS

General appearance

We found progressive local hair loss, skin swelling, and redness in the radiated side of the head of all experimental rats within 1–3 months after irradiation. All the rats showed slight loss of body weight within 1 month after irradiation and slow weight gain after 3 months after irradiation, which could be

attributed to poor eating and drinking in the first few months after radiation treatment. Fortunately, all these rats completed the MRI studies at all time points. All the MRI data were collected in the period from the starting time (preradiation) to the 9th month for the subsequent statistical analysis.

Magnetic resonance imaging findings

All MRIs were reviewed for detectable lesions or image abnormalities. No noticeable difference in image intensities was observed in the T2WI of any rat brain. As an *in vivo* approach, MRS was used for the identification of metabolic changes in the hippocampus region of brain. MRS voxels were positioned in the same brain region of all rats as far as possible [Figure 1]. The peak of NAA measure significantly decreased in the first 5 months after radiation treatment and then increased in the irradiated side. Conversely, the Cho and Cr levels significantly increased in the first 3 months and then decreased 5 months after radiation [Figure 1].

For NAA/Cr, repeated measurement data analysis result indicated that the factor of time (for two groups) interacting with the factor of groups had no statistical significance ($F = 1.47$, $P_g = 0.204$). However, there were significant differences ($P_g < 0.001$) between the radiation side and the contralateral side, taking all time points into consideration [Figure 2a]. Thus, the data underwent further statistical tests (multiple comparisons) with Bonferroni method for α correction. There were significant differences between the two groups in the 1st, 3rd, 5th, 7th, and 9th months after radiation treatment, but no statistical difference in the preradiation period (month 0) [Table 1]. Based on the paired *t*-test (within groups) results, there were significant differences in the brain hemisphere treated with irradiation between preradiation period and all the time points in the postradiation period. In the nonradiation side, there was no significant difference between preradiation period and each time point, except the 7th month after radiation treatment.

For NAA/Cho, repeated measurement data analysis result suggests a statistically significant interaction between time

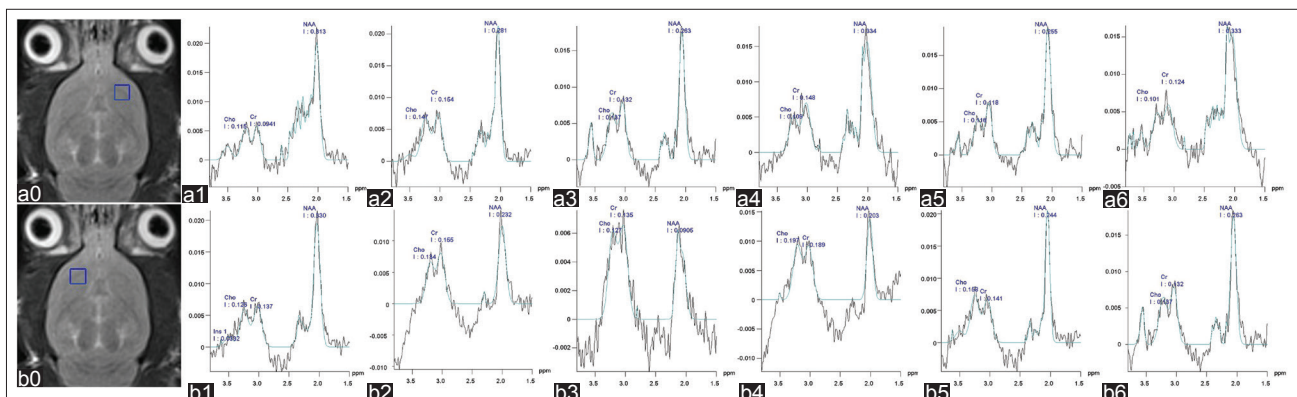


Figure 1: Volume of interest (VOI) with a voxel of 2.2 mm \times 2.2 mm \times 5.0 mm on irradiated side (b0) and control side (a0) on T2-weighted imaging (T2WI) for proton nuclear magnetic resonance spectroscopy. The spectral curves of a rat hippocampus before radiation treatment as well as the irradiated side (b1–b6) and control side (a1–a6) in the 0, 1st, 3rd, 5th, 7th, and 9th months after radiation treatment show that the peak of N-acetylaspartate (NAA) measure significantly decreased in the first 5 months after radiation treatment and then increased. Conversely, the choline (Cho) and creatinine (Cr) levels significantly increased in the first 3 months and then decreased after 5 months.

and group ($F = 4.72, P_{tg} < 0.001$). Under this circumstance, it should not only be seen in the integration of time points between group factors, but also be observed in the analysis of separate effects. Consequently, the data underwent further statistical tests (multiple comparisons) using Bonferroni method for α correction. There were significant differences between the two groups in the 1st, 3rd, 5th, 7th, and 9th months after radiation treatment and no statistical difference in the preradiation period (month 0) [Table 2 and Figure 2b]. According to paired t -test (within groups) results, there were significant differences in the brain hemisphere treated with irradiation between preradiation period and all the time points after radiation treatment. On the contrary, there was

no significant difference between the preradiation period and any time point after radiation treatment.

As for Cho/Cr, repeated measurement data (e.g., the ratio of NAA/Cho) analysis result shows that the factor of time (for two groups) interacting with the factor of groups had statistical significance ($F = 3.51, P_{tg} = 0.006$). As a result, the data underwent further statistical tests (multiple comparisons) using Bonferroni method for α correction. There were significant differences between the two groups only in the 3rd, 5th, and 7th months after radiation treatment, while there was no statistical difference in month 0, as well as in the 1st and 9th months [Table 3 and Figure 2c].

Table 1: Comparisons of NAA/Cr ratio at different time points ($n = 12$)

Time points	NAA/Cr				F	P_m	P_g	P_t	P_{tg}
	Control	P	Irradiated	P					
Pre-RT	2.89 ± 0.42	–	2.59 ± 0.32	–	0.521	0.057	<0.001	<0.001	0.204
Month 1	2.51 ± 0.61	0.035	1.49 ± 0.45	<0.001	1.594	<0.001			
Month 3	2.06 ± 0.78	0.010	1.24 ± 0.34	<0.001	10.901	0.003			
Month 5	2.36 ± 0.72	0.024	1.44 ± 0.60	<0.001	0.996	0.003			
Month 7	2.32 ± 0.52	0.001	1.26 ± 0.46	<0.001	0.145	<0.001			
Month 9	2.78 ± 0.75	0.454	1.91 ± 0.65	0.006	0.162	0.006			

All data were expressed as mean ± SD. P : P value for multiple comparisons using paired t -test (within groups); P_m : P value for multiple comparisons using t -test (between groups). Bonferroni method was used for multiple comparisons. t -tests were considered statistically significant when $P < 0.008$ (0.05/6). P_g : P value for between-groups effect; P_t : P value for within-subjects effect over time; P_{tg} : P value for interaction of time and group. RT: Radiation therapy; NAA: N-acetylaspartate; Cr: Creatinine; SD: Standard deviation.

Table 2: The ratio of NAA/Cho values at different time points in rats ($n = 12$)

Time points	NAA/Cho				F	P_m	P_g	P_t	P_{tg}
	Control	P	Irradiated	P					
Pre-RT	2.80 ± 0.54	–	2.73 ± 0.41	–	2.226	0.745	<0.001	<0.001	0.001
Month 1	2.70 ± 0.61	0.603	1.49 ± 0.65	<0.001	0.012	<0.001			
Month 3	2.42 ± 0.74	0.131	1.22 ± 0.40	<0.001	6.414	<0.001			
Month 5	2.43 ± 0.77	0.070	1.44 ± 0.58	<0.001	0.779	0.002			
Month 7	2.73 ± 0.57	0.648	1.25 ± 0.48	<0.001	1.014	<0.001			
Month 9	2.74 ± 0.64	0.799	1.87 ± 0.62	0.001	0.003	0.003			

All data were expressed as mean ± SD. P : P value for multiple comparisons using paired t -test (within groups); P_m : P value for multiple comparisons using t -test (between groups). Bonferroni method was used for multiple comparisons. t -tests were considered statistically significant when $P < 0.008$ (0.05/6). P_g : P value for between-groups effect; P_t : P value for within-subjects effect over time; P_{tg} : P value for interaction of time and group. RT: Radiation therapy; NAA: N-acetylaspartate; Cho: Choline; SD: Standard deviation.

Table 3: The ratio of Cho/Cr values at different time points in rats ($n = 12$)

Time points	Cho/Cr				F	P_m	P_g	P_t	P_{tg}
	Control	P	Irradiated	P					
Pre-RT	0.99 ± 0.19	–	0.94 ± 0.15	–	0.838	0.444	0.005	0.593	0.006
Month 1	0.91 ± 0.18	0.114	1.09 ± 0.20	<0.001	0.338	0.034			
Month 3	0.85 ± 0.12	0.087	1.06 ± 0.10	0.001	0.509	<0.001			
Month 5	0.89 ± 0.14	0.139	1.09 ± 0.11	0.010	0.683	0.001			
Month 7	0.85 ± 0.16	0.034	1.05 ± 0.15	0.100	0.012	0.005			
Month 9	0.95 ± 0.21	0.553	1.05 ± 0.18	0.039	0.004	0.246			

All data were expressed as mean ± SD. P : P value for multiple comparisons using paired t -test (within groups); P_m : P value for multiple comparisons using t -test (between groups). Bonferroni method was used for multiple comparisons. t -tests were considered statistically significant when $P < 0.008$ (0.05/6). P_g : P value for between-groups effect; P_t : P value for within-subjects effect over time; P_{tg} : P value for interaction of time and group. RT: Radiation therapy; Cho: Choline; Cr: Creatinine; SD: Standard deviation.

In accordance to the paired *t*-test of Cho/Cr, there were significant differences in the irradiated hemisphere between the preradiation period and the time points in the 1st and 3rd months after radiation treatment. Similarly, there was no significant difference between preradiation and any time point after radiation treatment.

Histologic findings

Four experimental rats were sacrificed for the histopathological evaluation after the final (in the 9th month after radiation) MRI scans. Both the gross morphology and the HE sections did not show obvious necrosis in the four rat brains. In the HE sections, the ipsilateral fimbria of the hippocampus demonstrated more neuronal damage, neuronal cell apoptosis, and neuronal dysfunction than the contralateral side. Through IHC staining of GFAP, astrocyte hypertrophy and hyperplasia of the astrocytes at the site of the hippocampus in the irradiated brain were seen and disorganized myelin fibers were also observed. In contrast, there was no significant histopathological alteration in the nonirradiated hemisphere [Figure 3a–3d].

DISCUSSION

Radiation therapy is an effective treatment for head and neck tumor. With proper radiation schemes, the 5-year survival rate of patients can be increased. Nonetheless, radiation-induced brain injury remains a clinical challenge.^[2,3] Radiation-induced brain injury may be reflected by many kinds of clinical symptoms, including nausea, emesis, headaches, and even cognitive dysfunction.^[1,11] In consequence, the accurate and timely diagnosis of radiation-induced brain injury is very important for proper therapy.

In this study, the radiation brain injury model of rats in one side of brain hemisphere was successfully established using single-dose exposure for long-term brain tissue monitoring after radiation. The radiation-induced brain injury in rat hemisphere model was observed *in vivo* at multiple time points, and the observation time was comparably longer. Metabolites changed dynamically over time in the MRS,

whereas no noticeable difference in image intensity was observed in the regular MRI. The findings were in agreement with a study result that ¹H MRI could effectively detect metabolic changes following radiation.^[4,6]

The dynamical alternation of metabolites might reflect the physiological changes of radiation-induced brain injury, which was a complicated course. The NAA/Cho and NAA/Cr ratios decreased in the first few months and slowly increased later. Nevertheless, they could not fully recover to the levels in the preradiation period. It might mean that the radiation-induced brain injury had an irradiated injury-recovering period.

NAA was considered to be a marker of neuronal density and function. Regional volume changes might result in a decrease of the NAA concentration due to neuronal damage, neuronal cell apoptosis, and neuronal dysfunction.^[4] This was consistent with our histological findings. An increase in water content caused by edema and myelination might also contribute to the changes in NAA values.^[6,12] The changing trends of NAA/Cr ratios in both sides (the control and radiation sides) were similar over time, which could be due to the influence of the scattering line on the contralateral brain tissue or the effect of the irradiated side on the whole-brain functional connection.

The Cho compound was associated with the cell membrane biosynthesis and metabolic turnover in proliferative tissue. Under pathological conditions, Cho may be released from phosphatidylcholine. During the first few months after radiation therapy, Cho increased and a significant decrease in the NAA/Cho ratio in brain tissue occurred in the 4th month after irradiation.^[2,6,13] Therefore, low NAA/Cho ratios might be due to early radiation-induced inflammation, demyelination, or gliosis which could decrease over time.^[14,15] As a marker of energy metabolism, Cr is normally considered to be stable under most conditions even if some reports have questioned the stability of Cr in tumors, hypoxia, and other confounding states.^[16]

In a 3D-echo-planar spectroscopic imaging experiment, the Cho/Cr ratio significantly increased in an area

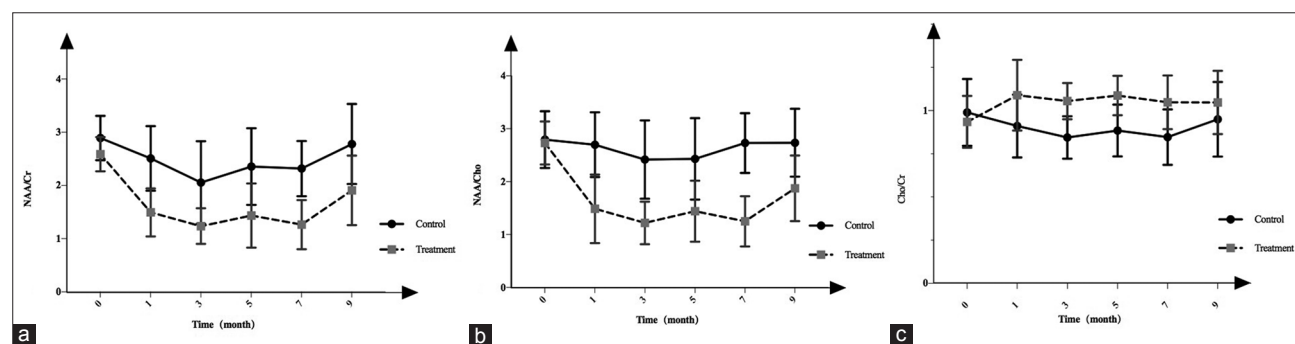


Figure 2: Longitudinal changes of the NAA/Cr, NAA/Cho, and Cho/Cr ratios at the different time points in the both hippocampus region. (a) In the irradiated hemispheres, the NAA/Cr ratio showed a rapid decrease after radiation and sustained decline in the first 3 months and then a gradual increase. In nonirradiated side, the NAA/Cr ratio had no significant changes in each time point. (b) The NAA/Cho ratio showed a rapid decrease during the initial 3 months followed by a gradual recovery in the irradiated side and had no significant changes in the other side. (c) The Cho/Cr in the hippocampus, there was no rapid increase or decrease in both sides. NAA: N-acetylaspartate; Cr: Creatinine; Cho: Choline.

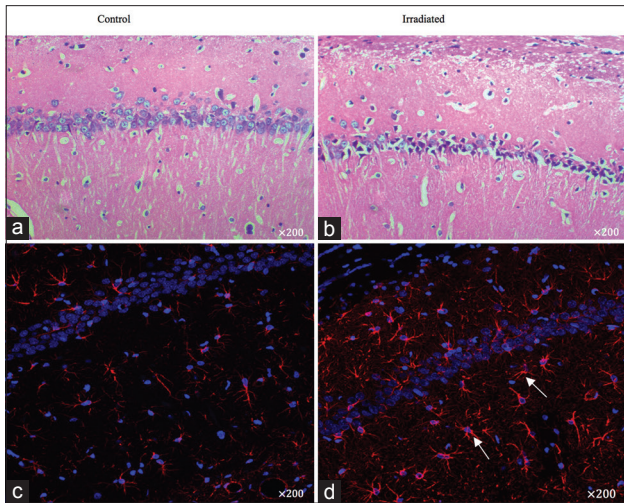


Figure 3: Histopathological evaluations of the irradiated (b and d) and nonirradiated (a and c) sides of a rat hippocampus at 9-month postirradiation, including H and E (a and b) and immunohistochemistry glial fibrillary acidic protein staining (c and d). Compared with the contralateral side, obvious pathologic changes, including neuronal damage and hypertrophy (arrow) and hyperplasia of astrocytes (red markers), were found in the irradiated side.

affected by radiation-induced injury, while NAA/Cr in the hippocampus decreased.^[16,17] In this study, the Cho/Cr ratio increased significantly in the 3rd, 5th, and 7th months after radiation treatment in the irradiated side, compared with the contralateral side. The higher Cho/Cr ratio suggests the occurrence of gliosis in the irradiated zone, which supports the hypothesis that glial cell injury occurred.^[18,19] It might also be reflected by the demyelination of the involved WM structures and membrane disruption associated with inflammation.^[19] These findings were consistent with our observations in GFAP staining.

In this study, the minimum value of NAA/Cho and NAA/Cr ratios in the irradiated hemisphere occurred in the 3rd month after radiation treatment. Nevertheless, the NAA/Cho and NAA/Cr ratios were close to their corresponding values in the preradiation period in the 9th month. Similar temporal changes in the NAA/Cho and NAA/Cr ratios have been observed in some studies on human. Sundgren *et al.*^[4] reported that NAA/Cr decreased significantly in the 3rd week after radiotherapy in their study. In the 1st and 6th months after radiotherapy, they got closer to their corresponding values in the preradiation period. Xiong *et al.*^[5] reported that the NAA/Cho and NAA/Cr ratios decreased significantly within 1 year after radiotherapy in their study. The decrease was the greatest in 0–3 months after radiation. After 12 months, the NAA/Cho and NAA/Cr ratios were close to the values observed in the preradiation period. The variations in metabolism may be due to the radiation-induced neuronal damage, the neuroinflammatory response triggered in microglial cells, as well as the blood-brain barrier disruption and repair processes.^[20,21]

Other studies reported that abnormalities in regular MRI were detected as early as 1–6 months after radiation.^[6,12] In

the current study, we found neither abnormal signal intensity in region treated with radiation in T2WI nor obvious brain necrosis both in the gross morphology and HE sections in the 9th month after irradiation of the sacrificed rats. This might be explained by the smaller exposure of hemi-brain to radiation, the compensatory effect of contralateral normal brain tissue, and the limited observation time.

However, there were several limitations in our study. First, the number of experimental rats was small, resulting in a lack of adequate histopathological comparisons with MRI at each time point. Second, only a single-dose radiation exposure was applied in the current study. Multi-dose radiation exposure should be utilized in further studies. Besides, dose response and dose-specific changes should be observed and understood. Third, the significant changes of NAA/Cr ratio in the side treated with no radiation in the 7th month might be considered as a drawback of the hemi-brain irradiation design.

In conclusion, the results of this study showed that ¹H-MRS was sensitive enough to detect metabolic alternations, which provided an opportunity to acquire brain metabolite information. The significant changes of metabolite ratio in the first few months after radiation treatment reflected metabolic disturbance in the acute and early delayed stages of radiation-induced brain injuries. The result might provide a basis for further investigations on the early detection and mitigation strategies for radiation-induced injury.

Financial support and sponsorship

The research was supported by grants from the Science and Technology Council of Shanghai (No. 15ZR1408000, and No. 12140901302), and Shanghai Municipal Commission of Health and Family Planning (No. 201440287).

Conflicts of interest

There are no conflicts of interest.

REFERENCES

- Zheng Q, Yang L, Tan LM, Qin LX, Wang CY, Zhang HN. Stroke-like migraine attacks after radiation therapy syndrome. *Chin Med J* 2015;128:2097-101. doi: 10.4103/0366-6999.161393.
- Wang HZ, Qiu SJ, Lv XF, Wang YY, Liang Y, Xiong WF, *et al.* Diffusion tensor imaging and ¹H-MRS study on radiation-induced brain injury after nasopharyngeal carcinoma radiotherapy. *Clin Radiol* 2012;67:340-5. doi: 10.1016/j.crad.2011.09.008.
- Chan AT. Nasopharyngeal carcinoma. *Ann Oncol* 2010;21 Suppl 7:vii308-12. doi: 10.1093/annonc/mdq277.
- Sundgren PC, Nagesh V, Elias A, Tsien C, Junck L, Gomez Hassan DM, *et al.* Metabolic alterations: A biomarker for radiation-induced normal brain injury-an MR spectroscopy study. *J Magn Reson Imaging* 2009;29:291-7. doi: 10.1002/jmri.21657.
- Xiong WF, Qiu SJ, Wang HZ, Lv XF. ¹H-MR spectroscopy and diffusion tensor imaging of normal-appearing temporal white matter in patients with nasopharyngeal carcinoma after irradiation: Initial experience. *J Magn Reson Imaging* 2013;37:101-8. doi: 10.1002/jmri.23788.
- Li H, Li JP, Lin CG, Liu XW, Geng ZJ, Mo YX, *et al.* An experimental study on acute brain radiation injury: Dynamic changes in proton magnetic resonance spectroscopy and the correlation with histopathology. *Eur J Radiol* 2012;81:3496-503. doi: 10.1016/j.ejrad.2012.03.011.

7. Shen CY, Tyan YS, Kuo LW, Wu CW, Weng JC. Quantitative evaluation of rabbit brain injury after cerebral hemisphere radiation exposure using generalized q-sampling imaging. *PLoS One* 2015;10:e0133001. doi: 10.1371/journal.pone.0133001.
8. Liu Y, Xiao S, Liu J, Zhou H, Liu Z, Xin Y, *et al.* An experimental study of acute radiation-induced cognitive dysfunction in a young rat model. *AJNR Am J Neuroradiol* 2010;31:383-7. doi: 10.3174/ajnr.A1801.
9. Kennedy AS, Archambeau JO, Archambeau MH, Holshouser B, Thompson J, Moyers M, *et al.* Magnetic resonance imaging as a monitor of changes in the irradiated rat brain. An aid in determining the time course of events in a histologic study. *Invest Radiol* 1995;30:214-20.
10. Chan KC, Khong PL, Cheung MM, Wang S, Cai KX, Wu EX. MRI of late microstructural and metabolic alterations in radiation-induced brain injuries. *J Magn Reson Imaging* 2009;29:1013-20. doi: 10.1002/jmri.21736.
11. Bhakoo KK, Pearce D. *In vitro* expression of N-acetyl aspartate by oligodendrocytes: Implications for proton magnetic resonance spectroscopy signal *in vivo*. *J Neurochem* 2000;74:254-62. doi: 10.1046/j.1471-4159.2000.0740254.x.
12. Sundgren PC. MR spectroscopy in radiation injury. *AJNR Am J Neuroradiol* 2009;30:1469-76. doi: 10.3174/ajnr.A1580.
13. Young GS. Advanced MRI of adult brain tumors. *Neurol Clin* 2007;25:947-73, viii. doi: 10.1016/j.ncl.2007.07.010.
14. Verma N, Cowperthwaite MC, Burnett MG, Markey MK. Differentiating tumor recurrence from treatment necrosis: A review of neuro-oncologic imaging strategies. *Neuro Oncol* 2013;15:515-34. doi: 10.1093/neuonc/nos307.
15. Rutkowski T, Tarnawski R, Sokol M, Maciejewski B. ¹H-MR spectroscopy of normal brain tissue before and after postoperative radiotherapy because of primary brain tumors. *Int J Radiat Oncol Biol Phys* 2003;56:1381-9. doi: 10.1016/S0360-3016(03)00327-4.
16. Chuang MT, Liu YS, Tsai YS, Chen YC, Wang CK. Differentiating radiation-induced necrosis from recurrent brain tumor using MR perfusion and spectroscopy: A meta-analysis. *PLoS One* 2016;11:e0141438. doi: 10.1371/journal.pone.0141438.
17. Kaminaga T, Shirai K. Radiation-induced brain metabolic changes in the acute and early delayed phase detected with quantitative proton magnetic resonance spectroscopy. *J Comput Assist Tomogr* 2005;29:293-7. doi: 10.1097/01.rct.0000161422.95625.8a.
18. Chawla S, Wang S, Kim S, Sheriff S, Lee P, Rengan R, *et al.* Radiation injury to the normal brain measured by 3D-echo-planar spectroscopic imaging and diffusion tensor imaging: Initial experience. *J Neuroimaging* 2015;25:97-104. doi: 10.1111/jon.12070.
19. Shutter L, Tong KA, Lee A, Holshouser BA. Prognostic role of proton magnetic resonance spectroscopy in acute traumatic brain injury. *J Head Trauma Rehabil* 2006;21:334-49. doi: 10.1097/00001199-200607000-00005.
20. Rana P, Khan AR, Modi S, Hemanth Kumar BS, Javed S, Tripathi RP, *et al.* Altered brain metabolism after whole body irradiation in mice: A preliminary *in vivo* ¹H MRS study. *Int J Radiat Biol* 2013;89:212-8. doi: 10.3109/09553002.2013.734944.
21. Matulewicz L, Sokól M, Michnik A, Wydmanski J. Long-term normal-appearing brain tissue monitoring after irradiation using proton magnetic resonance spectroscopy *in vivo*: Statistical analysis of a large group of patients. *Int J Radiat Oncol Biol Phys* 2006;66:825-32. doi: 10.1016/j.ijrobp.2006.06.001.